Research

Bacterial Deposition in Porous Media Related to the Clean Bed Collision Efficiency and to Substratum Blocking by Attached Cells

HUUB H. M. RIJNAARTS,*,†
WILLEM NORDE,‡
EDWARD J. BOUWER,§
JOHANNES LYKLEMA,‡ AND
ALEXANDER J. B. ZEHNDER†,∥

Department of Microbiology, Wageningen Agricultural University, Hesselink van Suchtelenweg 4, 6703 CT Wageningen, The Netherlands, Department of Physical and Colloid Chemistry, Wageningen Agricultural University, Dreijenplein 6, 6703 HB Wageningen, The Netherlands, and Department of Geography and Environmental Engineering, The Johns Hopkins University, Baltimore, Maryland 21218

Deposition of *Pseudomonas putida* mt2 and *Rhodococcus* strain C125 during transport through columns packed with Teflon grains was investigated. Deposition was analyzed in terms of the clean bed collision efficiency α_0 (the probability of a cell to attach upon reaching a cell-free substratum) and the surface area blocked by attached cells. Blocking was quantified by a blocking factor B, the ratio of the blocked area per cell to the geometric area of a cell. At an average interstitial fluid velocity of 200 μm s^{-1}, α_0 is close to unity (0.83 ± 0.01) for both strains, indicating that cell−solid interactions are almost completely favorable for deposition. Values for B of 1.6 ± 0.1 and 12.0 ± 0.8 were obtained for *Ps. putida* and *Rhodococcus* strain C125, respectively. This difference is consistent with differences in cell size and cell−cell repulsion, which were both smaller for *Ps. putida* than for *Rhodococcus* strain C125. At coverages close to saturation, multilayer adhesion and/or pore clogging occurs for the weakly blocking *Pseudomonas* cells but not for the strongly blocking *Rhodococcus* cells. The collision-blocking concept succesfully explains the breakthrough of *Bacillus* cells in coarse sand columns, as reported by Lindqvist and Enfield, for which adhesion is less favorable ($\alpha_0 = 0.10 ± 0.01$) and blocking is relatively strong ($B = 5.8 ± 0.8$). The general

conclusion is that deposition of microbes during their transport through coarse grain media is adequately described by the collision-blocking model in cases of strongly blocking cells or weakly blocking cells at low coverage conditions.

Introduction

Bioremediation of contaminated soil and groundwater is based on a stimulation of the dispersal and the activity of indigenous or introduced bacteria (*1−3*). On the other hand, high numbers of mobile microorganisms in groundwater can also cause unwanted effects such as a contamination of drinking water resources with microbes (*4, 5*) and/or with chemicals mobilized by biocolloid facilitated transport (*5, 6*). Hence, a control of bacterial transport in porous media is required for safe and effective bioremediation. Bacterial transport has been modeled in terms of deposition and detachment, particle capture by straining (mechanical filtering eventually leading to pore clogging) and particle release from clogged pores (*7−13*). These models and their mechanistic pre-assumptions were generally not validated (*14*). The present study aims to provide a better basis for bacterial transport modeling by identifying and quantifying the principal mechanisms of bacterial retention in coarse grain media. For this purpose, column breakthrough experiments with well-characterized Teflon collectors and bacterial strains were performed. In addition, literature data on bacterial transport in coarse sand media were analyzed.

Theory

Deposition is the only process controlling the initial cell removal from the fluid phase during transport in coarse grain media, because (i) the bacterial radius a_b (m) is much less than the grain radius a_s (m), so that straining is excluded ($N_R = a_b/a_s \ll 0.05$) (*15, 16*), and (ii) detachment is insignificant since bacterial deposition is generally irreversible (*17, 18*). Deposition is determined by two processes: (i) the transfer of particles from bulk water to the grain (collector) surface and (ii) adhesion. Colloid filtration theory was used to quantify these two processes in terms of the collector mass transfer efficiency η (the probability of a particle approaching a collector to reach its surface) and the adhesion or collision efficiency α (the probability of a particle to attach upon reaching the surface) (*15, 16, 19, 20*).

The value of η was calculated as follows (15, 16, 21):

$$\eta = 4A_s^{1/3}N_{Pe}^{-2/3} + A_sN_{vdw}^{1/8}N_R^{15/8} +$$
$$0.00338A_sN_G^{1.2}N_R^{-0.4} \quad (1)$$

Here, $A_s = 2(1 - p^5)/[2 - 3p + 3p^5 - 2p^6]$, $p = (1 - \epsilon)^{1/3}$, and ϵ is the porosity of the column to account for the effect of neighboring collectors. The dimensionless numbers N are indicative of the various contributions to η: the Peclet number $N_{Pe} = 2Ua_s/D_b$ for the sum of convection and diffusion, $N_R = a_b/a_s$ for interception (particles collide with the surface because of their size) and hydrodynamic retardation due to viscous drag at close proximity of the collector surface, $N_G = 2a_b^2(\rho_p - \rho)g/[9\mu U]$ for sedimentation, and $N_{vdw} = A_{bs(w)}/[9\pi a_b^2 U]$ for acceleration of mass transfer as a result of van der Waals attraction. The parameters in these formulations of N are defined as follows: U (m s^{-1}) is the velocity of the fluid phase that enters the column, D_b (m^2 s^{-1}) is the diffusion coefficient of the bacterium, ρ_b and ρ (kg m^{-3}) are the densities of the bacterium and fluid phase, respectively, μ (kg m^{-1} s^{-1}) is the dynamic viscosity of the fluid phase, and $A_{bs(w)}$ (J) is the Hamaker constant for van der Waals interaction between a bacterium (b) and the solid phase (s) across the medium water (w). The first term on the right hand side of eq 1 describes the contribution of convection and diffusion to η while the other terms account for direct interception and deviation from trajectories due to the other influences. For a detailed description of eq 1, the reader is referred to refs 15, 16, and 21.

The level of α is controlled by cell−solid interactions (17, 22, 23) and by the amount of previously attached bacteria. An attached (bacterial) particle can reduce deposition by blocking a part of the collector surface (18, 24−28). An expression for the influence of cell−solid interactions and cell-cell interactions (blocking) on α becomes (25, 27)

$$\alpha = \alpha_0(1 - B\Theta) \quad (2)$$

where α_0 is the clean bed collision efficiency, B is the blocking factor, and Θ is the fraction of surface covered, i.e., number of cells m^{-2} × πa_b^2. Initially, $\Theta = 0$ and α is solely determined by cell−solid interactions ($\alpha = \alpha_0$); $\alpha_0 = 1$ when these interactions do not inhibit the adhesion step. B accounts for the screening of the solid surface by attached cells, i.e., it is the ratio of the blocked area to the geometric area of the cell. It is related to the maximum surface coverage Θ_{max} for single layer adhesion: $\Theta_{max} = 1/B$. The B factor may vary between 1.5 to more than 20 and depends on geometric/hydrodynamic parameters a_b and N_{Pe} and particle−particle interactions (24, 26, 28, 29).

The deposition rate at any position in the porous bed can be expressed as change in either the suspended particle concentration c or Θ:

$$-\frac{dc}{dt} = G\frac{d\Theta}{dt} = k\alpha_0(1 - B\Theta) \quad (3)$$

where $G = 3(1/\epsilon - 1)/(\pi a_s a_b^2)$ and mass transfer coefficient k (s^{-1}) is defined as $k = 3/4(1/\epsilon - 1)U\eta/a_s$. Analytical solutions of this equation exist for semi-steady-state conditions, i.e., initial breakthrough has occurred and tailing effects due to hydrodynamic dispersion have died away. In case of negligible blocking ($B = 0$, $\alpha = \alpha_0$), c is constant with time at given porous medium depth L (m) and declines

with L according to (30)

$$c = c_0e^{-\lambda L} \quad (4)$$

Here, c_0 is the influent cell concentration and λ (m^{-1}) is the filter coefficient that is coupled to $\eta\alpha$ according to

$$\lambda = 3/4[(1 - \epsilon)/a_s]\eta\alpha \quad (5)$$

In case of blocking ($B > 0$), c at given L becomes a function of time (31):

$$\frac{c}{c_0} =$$
$$\frac{\exp(1/4\pi a_b^2 Uc_0\eta\alpha_0Bt^*)}{\exp(3/4(1 - \epsilon)/a_s\eta\alpha_0) + \exp(1/4\pi a_b^2 Uc_0\eta\alpha_0Bt^*) - 1} \quad (6)$$

where $t^* = t -$ column hydraulic retention time.

The equations above apply to single-layer adhesion, i.e., eventually the surface becomes saturated and completely blocked for further deposition (α(coating) = 0). Other formulations are needed to describe multilayer adhesion (α(coating) > 0), which leads to enhanced particle removal (filter ripening) by straining and pore-clogging (29, 31, 32).

Materials and Methods

Bacteria. Two bacterial species were investigated, namely, *Pseudomonas putida* mt2 and *Rhodococcus* strain C125. Sources, procedures for cultivation and preparation, and cell surface properties of these bacteria were described elsewhere (22). The geometric mean radius a_b and diffusion coefficient D_b are 0.59 ± 0.07 μm and (3.65 ± 0.05) × 10^{-13} m^2 s^{-1}, respectively, for *Ps. putida*, and 1.17 ± 0.37 μm and (1.74 ± 0.03) × 10^{-13} m^2 s^{-1}, respectively, for *Rhodococcus* C125. The bacteria differ in electrostatic properties; at an ionic strength of 0.1 M, the ζ-potentials are −50 and −10 mV for *Rhodococcus* C125 and *Ps. putida*, respectively (17).

Aqueous Media, Collectors, and Columns. Phosphate-buffered saline solution (PBS) with an ionic strength of 0.1 M and a pH of 7.2 (22) was used for all experiments. Spherical collectors of PFA−Teflon, previously described (22), and of PTFE (Fluorplast, Raamsdonksveer, The Netherlands) were used. Procedures for cleaning the collectors and packing the columns are described elsewhere (22). The dimensions of collectors and the glass columns are given in Table 1. Total porosity values and pore volumes of PFA-packed columns were estimated from breakthrough curves using chloride as the conservative tracer and by gravimetry. Chloride concentrations were measured with a microchlorocounter (Marius, Utrecht, The Netherlands).

Column Experiments. Experiments were done with vertical down-flow columns. Bacterial suspensions in PBS

List of Experiments, Flow Rates Q at Which Suspensions Were Applied, Column Lengths L, and Hydraulic Retention Times t_{HR} (V_{col}/Q) of Columns Used

experiment	bacterium/collector	Q (cm^3 h^{-1})	L (cm)	t_{HR} (min)
1. reproducibility test	*Ps. putida*/PFA	19.0 ± 0.5	7.5	6.3
2. reproducibility test	*Rhodococcus* C125/PFA	14.9 ± 0.3	8.9	12.2
3. effect of column length	*Ps. putida*/PFA	20.0 ± 0.5	2.5	2.0
			4.8	3.8
			7.5	6.3
			12.0	9.8
4. effect of column length and flow rate		21.6 ± 0.5	3.3	2.4
			5.0	3.7
4A	*Rhodococcus* C125/PFA		7.5	5.6
			13.6	10.0
4B	*Rhodococcus* C125/PFA	12.2 ± 0.6	4.3	6.0
			9.8	12.3
			13.0	17.0
4C	*Rhodococcus* C125/PFA	4.2 ± 0.3	2.9	10.3
			4.5	16.6
			7.5	31.5
			13.6	52.0
5. large collectors	*Rhodococcus* C125/PTFE	74.6 ± 1.5	25.2	29.8

with an optical density at 280 nm (OD$_{280}$) of 0.6 were prepared by diluting samples of concentrated stock suspensions. The resulting suspensions with a cell concentration c_0 of 5.3×10^8 cells cm^{-3} for *Ps. putida* and 3.6×10^7 cells cm^{-3} for *Rhodococcus* C125 were applied to the columns by means of a peristaltic pump. The effluent cell concentration c, as measured by OD$_{280}$, was monitored with time. c_0 (OD$_{280}$) was found to be constant throughout the experimental time in all cases. The columns were operated for 2−4 h. The different experiments and specific conditions are listed in Table 2. Experiments 1 and 2 were performed in duplicate using independently grown and prepared cells for each column. A single column for each condition (flow rate, column length, collector size) was used in experiments 3−5.

Determination of α, α$_0$ and B. *Method 1.* The filter coefficient λ was estimated by linear regression analysis of the $\ln(c/c_0) - L$ data ($\ln(c/c_0) = -\lambda L$; eq 4) obtained from columns with different lengths L (experiments 3 and 4) using c-levels taken just after the initial breakthrough and at the end of the experiment. Values of α were calculated with eq 5, the measured values of λ, and the calculated levels of η (eq 1). The Hamaker constant $A_{bs(w)}$ for the Teflon−water−bacterium was set to 2×10^{-22} J (*17*) for calculating N_{vdw} (eq 1).

Method 2. The λ was measured as a function of time for every single column studied, by calculating $\ln(c/c_0)/L$ for each measured c value. The value of α was calculated following method 1. In addition, the average surface coverage Θ_{col}, defined as the number of deposited cells in the column times πa_b^2 divided by the porous medium surface area A_{col} in the column, was determined as a function of t by integrating the breakthrough curve. After a number of V pore volumes [$V = tQ/V_{col}$ where Q is the flow rate (m^3 s^{-1}), t is time (s), and V_{col} is the column pore volume (m^3)] have passed through the column, Θ_{col} is

$$\Theta_{col}(t) = V_{col}(-c_0 + \int_0^{V_{ss}} (c_0 - c)\, dV + \int_{V_{ss}}^{V(t)} (c_0 - c)\, dV)\pi a_b^2/A_{col} \quad (7)$$

where

$$V_{col}\left(-c_0 + \int_0^{V_{ss}} (c_0 - c)\, dV\right)$$

equals the number of cells deposited during the initial non-steady-state phase, and V_{ss} is the number of pore volumes beyond which a semi-steady-state exists. Finally, α$_0$ and B were estimated by fitting eq 2 to the $\alpha - \Theta_{col}$ data by a standard linear regression procedure.

Method 3. The values of α$_0$ and B were estimated by fitting eq 6 to the breakthrough data of the semi-steady-state period using standard nonlinear regression personal computer software.

In some cases, $\Theta(L,t)$ was estimated from λ_i values, determined from c levels measured at different time intervals Δt_i (method 2) according to

$$\Theta(L,t) = \frac{c_0 U}{G_2} \sum_{i=1}^{n} (\lambda_i e^{-\lambda_i L} \Delta t_i) \quad (8)$$

where $\Delta t_1 = t_1 - t_{L,0}$, $\Delta t_2 = t_2 - t_1$, ..., $\Delta t_n = t_n - t_{n-1}$ and $t_{L,0} = L\epsilon/U < t_1 < t_2, ... < t_n$.

Analysis of Literature Data on Bacterial Transport in Sand Columns. The data on the dispersal of *Bacillus* strain CB2 in columns with coarse (Texas) sand reported by Lindqvist and Enfield (*13*) were analyzed using the following system properties, in part given by these authors: $\epsilon = 0.34$, $Q = 34.3$ cm^3 h^{-1}, column diameter = 5 cm, $L = 5$ cm, $V_{col} = 33.6$ cm^3, the geometric mean estimate of the bacterial radius (*22*) $a_b = 1/2(1.9\ \mu m \times 0.7\ \mu m)^{1/2} = 0.58\ \mu m$, $a_s = 550 \pm 50\ \mu m$, a specific area for the sand of 21 cm^2 g^{-1}, i.e., $A_{col} = 0.36$ m^2, and $A_{bs(w)} = 6.2 \times 10^{-21}$ J, which is appropriate for glass and silica surfaces (*17*).

Results and Discussion

Column Results. *Reproducibility Tests.* The chloride tracer results of experiment 1 (not shown) and experiment 2 (Figure 1) indicate that effects of hydrodynamic dispersion were absent at $V > 2$, i.e., $V_{ss} = 2$ (eq 7). Breakthrough of cells occurred approximately after 1 pore volume (Figure
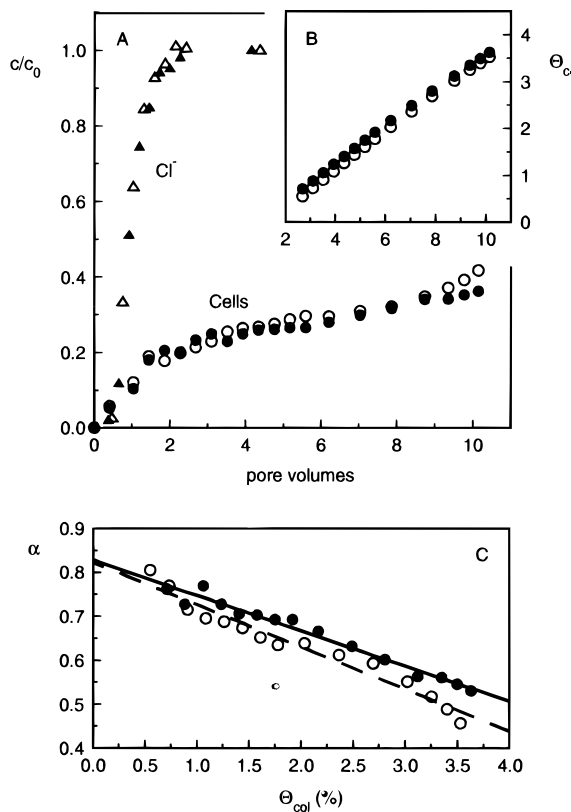
FIGURE 1. Check of reproducibility of breakthrough; results for *Rhodococcus* strain C125 and PFA collectors. (A) Breakthrough of cells (circles) and chloride (triangles). (B) The increase of the average surface coverage Θ_{col} with number of pore volumes fed. (C) The collision efficiency α as a function of average surface coverage; lines represent linear regression results. Open and filled symbols and solid and dashed lines indicate results of independent duplicate experiments.

1A), and initially about 80% of the cells deposited. Thereafter, the deposition decreased as indicated by (i) an increase of c/c_0 to about 0.4, (ii) a decrease of the slope of the $\Theta_{col}-V$ plots with increasing Θ_{col} (Figure 1B), and (iii) the decrease of α from initial (α_0) levels of 0.82 ± 0.01 (methods 2 and 3, Table 3) to values between 0.4 and 0.6 at Θ_{col} levels of about 4% for *Rhodococcus* C125 (Figure 1C) and at $\Theta_{col} =$ 20% for *Ps. putida* mt2 (not shown). The values of B (methods 2 and 3) indicate a great difference in blocking between the two strains and correspond to maximum coverages of 54–66% for *Ps. putida* and 9–11% for *Rhodococcus* C125 (Table 3). The good experimental reproducibility permitted the use of a single column for each subsequent condition investigated.

Effect of Column Length. The results obtained with *Ps. putida* (experiment 3) show that the fraction of cells removed from the fluid phase increases with column length (Figure 2A). At $t = 38$ min, c/c_0 decreased exponentially with bed length according to eq 4 (Figure 2B). However, λ and α (method 1), decreased by 25% over the period $t = 38$ min to $t = 113$ min (Figure 2B; Table 4). The $\alpha-\Theta_{col}$ plots (method 2, Figure 2C) show that α is initially about 0.8, then decreases with Θ_{col} for all columns, and finally levels off or slightly increases with Θ_{col}. For the two longest columns, the initial decrease was most pronounced and approximately linear with Θ_{col}. The average value of B (methods 2 and 3) of these columns is similar as for

experiment 1 (Table 3). The value for α increased with Θ at higher coverages for the two shortest columns, and linear regression gave poor results (not shown). The B values obtained with method 3 are independent on L for $L \geq 7.5$ (Table 5). The estimated variation of Θ (eq 8) between the column outlet and inlet was 14% < $\Theta(L)$ < 33% at $t = 53$ min for the 2.5-cm column and 16% < $\Theta(L)$ < 47% at $t = 97$ min for the 4.8-cm column. Apparently, multilayer adhesion and filter ripening significantly affect the retention of this bacterium at $\Theta > 0.5\Theta_{max}$ as reached in the upstream parts of the columns.

For *Rhodococcus* C125 (experiment 4A; Figure 3A–C), c decreased exponentially with L in the lower parts of the columns (Figure 3B) but the $\ln(c/c_0) - L$ regression lines intersected the L-axis at $L > 0$. Apparently, there was low or no deposition in the upper few centimeters of the columns. These low deposition zones became longer with time. Values of λ and α (method 1) decreased with time (Figure 3B; Table 4), indicating blocking. The α-values (method 2) obtained from the shortest columns were much smaller than those for the two longest columns (Figure 3C). The value of α determined by method 1 ($t = 38$ min; Table 4) is somewhat smaller than the α_0 value (methods 2 and 3) for the two longest columns (Figure 3C; Table 3). The B values obtained with these columns are similar to that of experiment 2 (Table 3) and are independent on L for $L \geq 7.5$ (Table 5). The estimated coverage at the top of the columns $\Theta(L = 0)$ was 4.9 ± 0.3% at $t = 38$ min and 8.1 ± 1% at $t = 113$ min. Considering $\Theta_{max} = 10 \pm 1\%$, the low deposition in the top layers of the columns most likely resulted from surface saturation by the strongly blocking attached cells.

Straining Test. Although straining is not likely to occur in the system used ($N_R = 0.006$), a column test with the larger PTFE beads and *Rhodococcus* C125 (experiment 5) was performed. The pores between the PTFE beads are much too large to permit straining ($N_R = 0.0007 \ll 0.05$). Except for a difference in α_0, B values for the PFA and PTFE columns are insignificantly different (Table 3). Therefore, blocking caused the decrease of α with increasing Θ_{col} for both types of Teflon collectors as well as the low deposition in the top of the PFA-packed columns.

Effect of Fluid Velocity. The level of c/c_0 for *Rhodococcus* C125 cells increases much slower with t and V for the lowest flow rate $Q = 4.3$ cm^3 h^{-1} (experiment 4C) in comparison to the highest flow rate $Q = 21.6$ cm^3 h^{-1} (Figure 3A). Values of α (method 1, Table 4) are smaller than α_0 (methods 2 and 3, Table 3) in all cases. Both α_0 and B decrease with average interstitial fluid velocity U/ϵ whereas the opposite is observed for B.

Comparison of Methods. The method 2 procedure of coupling α to surface coverage (Θ_{col}) is superior to estimation of λ and α from $\ln(c/c_0) - L$ plots (method 1) because it provides estimates of α_0 and B. Moreover, α obtained with method 1 is smaller than α_0 in all cases (Tables 3 and 4). Determination of α_0 and B with method 2 (Figures 2C and 3C) and method 3 (Table 5) requires a minimum column length L of 7.5 cm. Plotting α_0 against Θ_{col} (method 2) for different column lengths including $L < 7.5$ cm provides information about processes that occur at coverages close to surface saturation. Both methods 2 and 3 are suitable for analyzing column deposition results since they provide insignificantly different estimates of α_0 and similar B values (Table 3).

TABLE 3

Experimental Values of Clean Bed Collision Efficiency α_0, Blocking Factor B, and Maximum Coverage Θ_{max}, Determined According to Method 2 ($\alpha - \Theta_{col}$ Plot) and Method 3 (Analytical Solution, Eq 6)

experiment	strain/collector	method 2			method 3		
		α_0	B	Θ_{max}, (%)	α_0	B	Θ_{max} (%)
1	*Ps. putida*/PFA	0.82 ± 0.03	1.84 ± 0.22	54.3	0.82 ± 0.02	1.57 ± 0.16	63.7
3	*Ps. putida*/PFA	0.82 ± 0.03	2.00 ± 0.02	50.0	0.80 ± 0.03	1.52 ± 0.17	65.8
2	*Rhodococcus* C125/PFA	0.83 ± 0.01	10.61 ± 0.96	9.4	0.84 ± 0.01	9.43 ± 0.95	10.6
4A	*Rhodococcus* C125/PFA	0.81 ± 0.06	11.98 ± 0.72	8.3	0.81 ± 0.06	10.81 ± 0.15	9.3
4B	*Rhodococcus* C125/PFA	0.62 ± 0.04	10.0 ± 2.3	10.0	0.64 ± 0.04	9.5 ± 1.3	10.5
4C	*Rhodococcus* C125/PFA	0.55 ± 0.04	8.4 ± 5.3	12.0	0.59 ± 0.05	7.4 ± 2.4	13.5
5	*Rhodococcus* C125/PTFE	1.07 ± 0.10	11.0 ± 7.0	9	1.10 ± 0.10	10.0 ± 1.5	10.0
ref 13	*Bacillus* CB1/sand	0.098 ± 0.008	5.8 ± 0.8	17	0.101 ± 0.012	5.3 ± 0.7	19
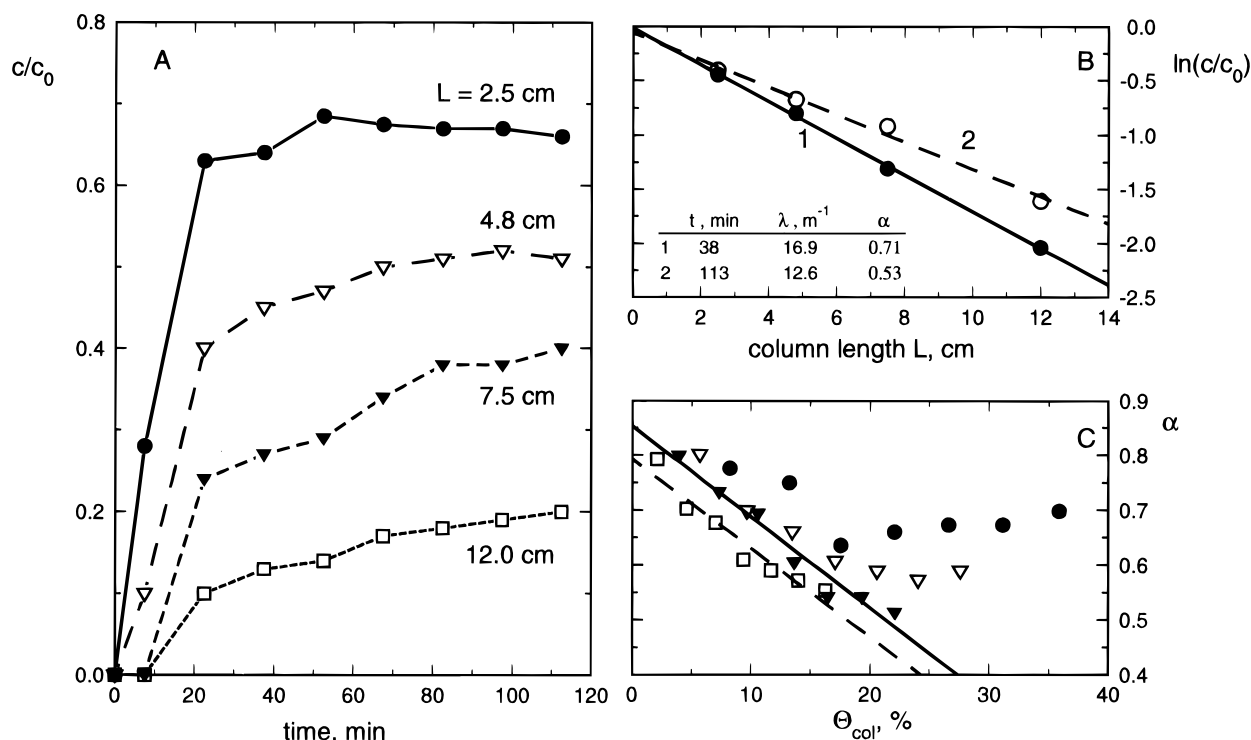
FIGURE 2. Results for *Pseudomonas putida* mt2 and PFA-packed columns with various lengths *L*. (A) Breakthrough profiles of the cells. (B) Plot of ln(c/c_0) as a function of column length at two times; lines indicate linear regression results. (C) The collision efficiency α as a function of average surface coverage Θ_{col}; lines represent linear regression results of the two longest columns.

TABLE 4

Filter Coefficient λ and Collision Efficiency α Derived from λ According to Method 1

experiment	strain/collector	λ (m^{-1})		α from $\lambda(t_1)$[a]
		t_1[a]	t_2[a]	
3	*Ps. putida*/PFA	16.9 ± 0.4	12.6 ± 1.0	0.71 ± 0.01
4A	*Rhodococcus* C125/PFA	12.8 ± 0.7	9.8 ± 0.5	0.74 ± 0.04
4B	*Rhodococcus* C125/PFA	11.2 ± 0.2	6.8 ± 2.4	0.47 ± 0.01
4C	*Rhodococcus* C125/PFA	23.9 ± 1.2	26.6 ± 1.3	0.52 ± 0.02

[a] t_1 = 38 min and t_2 = 113 min for experiments 3 and 4A; t_1 = 105 min and t_2 = 360 min for experiments 4B and 4C.

Mass Transfer Efficiency η. The value of η and the fraction of η determined by convection and diffusion increased with decreasing N_{Pe}, i.e., with decreasing U (experiments 2 and 4), decreasing cell size, and decreasing collector size (experiment 4A versus experiment 5) (Table 6). The fraction of η determined by convection and diffusion varied between 80 and 90% for *Rhodococcus* C125 cells and 97% for the relatively small cells of *Ps. putida*. Compared to *Ps. putida*, the larger size of *Rhodococcus* C125 cells results

in greater relative contributions of sedimentation and van der Waals attraction values (*15, 16*).

Factors Affecting α_0 and B. Values for α_0 of 0.82−0.83 observed for both bacterial species indicate close to favorable cell−solid interactions ($\alpha_0 = 1$), which confirms previous findings obtained with batch systems (*17, 22*). The increase of α_0 with N_{Pe} as observed for *Rhodococcus* C125 may be caused by shear forces helping these cells to surmount a small energy barrier during deposition on
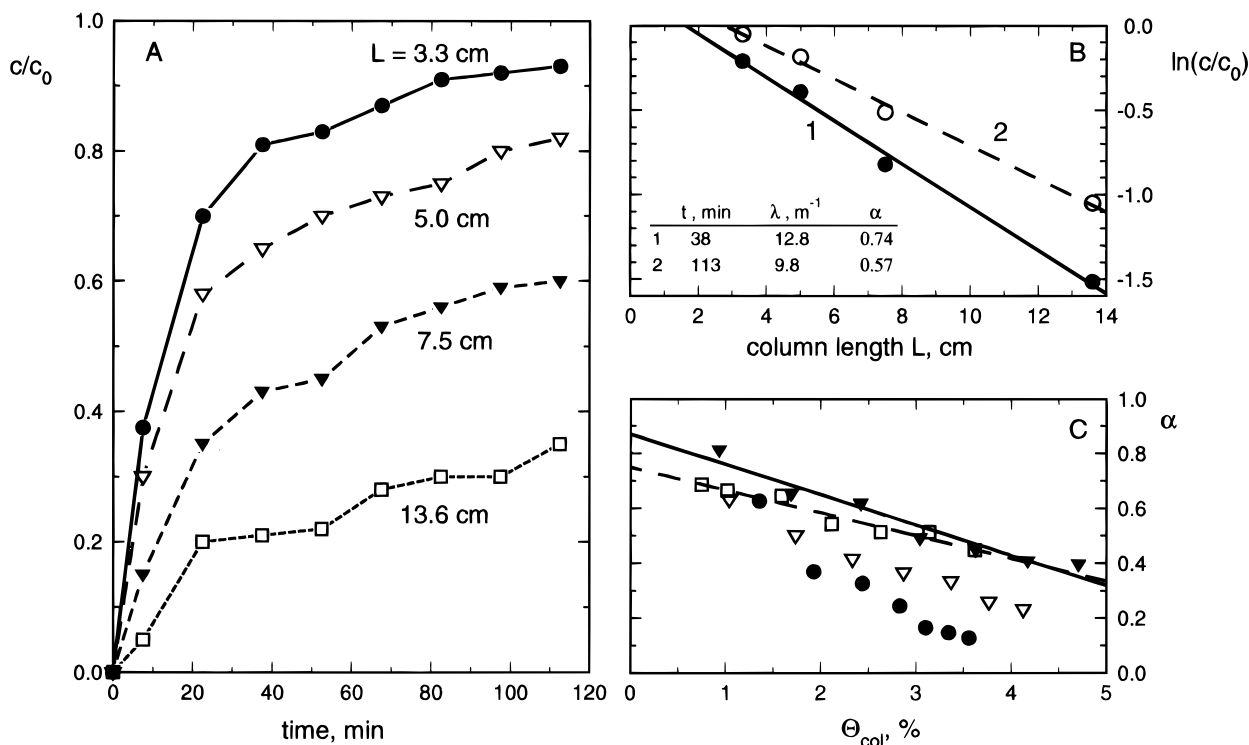
FIGURE 3. Results for *Rhodococcus* strain C125 and PFA-packed columns with various lengths *L*. Otherwise as in Figure 2.

Dependency of Blocking Factor B, as Estimated According to Method 3, on Column Length L for Pseudomonas putida mt2 and Rhodococcus C125

	L (cm)	*B*
Pseudomonas putida mt2	2.5	0.31 ± 0.21
	4.8	0.99 ± 0.16
	7.5	1.59 ± 0.17
	12.0	1.45 ± 0.15
Rhodococcus C125	3.3	22.5 ± 2.9
	5.0	15.1 ± 0.5
	7.5	11.4 ± 0.8
	13.6	10.2 ± 1.0

Teflon. A stimulation of deposition of *Rhodococcus* C125 and other cells by shear forces was observed in previous studies (*17, 22*).

The blocking factor *B* differs strongly between the two bacterial strains at comparable fluid velocity (experiments 1, 3, and 4A; Table III). *B* factors for *Ps. putida* correspond to Θ_{max} values close to the theoretical upper limit of 54% (*24*). On the other hand, the lowest Θ_{max} of 8.3% (*Rhodococcus* C125, $B \approx 12$; Table 3) is not an exceptional value (*18, 25, 27, 28*). The dissimilarity in *B* between the two strains can at least partially be explained by the difference in a_b and N_{Pe}. *Ps. putida* cells are smaller than those of *Rhodococcus* C125 and therefore exhibit a smaller N_{Pe} value at the same flow rate (Table 6). As a consequence, they have a smaller hydrodynamic "shadow" (Figure 5A,B), i.e., they diffuse faster, approach the collector surface in steeper trajectories, and are less hindered by the attached cells than *Rhodococcus* C125. The experiments with *Rhodococcus* C125 cells demonstate that *B* increases with increasing N_{Pe}, i.e., with increasing U/ϵ (experiment 4A–C) or collector size (experiment 5) (Tables 3 and 4). These findings are

consistent with results reported for polystyrene particles (*26*) and can also be qualitatively understood in terms of the shadow effect (Figure 5B,C): decreasing N_{Pe} values give steeper trajectories and a reduced blocking.

Factors having a nonhydrodynamic/geometric origin also contribute to blocking: for *Rhodococcus* C125 cells at $N_{Pe} = 3.3 \times 10^{-4}$ (experiment 4c), *B* is more than a factor of 4 higher than for *Ps. putida* at $N_{Pe} = 7.2 \times 10^{-4}$ (experiments 1 and 3) (Table 3). One of these factors may be a different extent in cell–cell electrostatic repulsion. At an ionic strength of 0.1 M, double-layer repulsion is screened and (electro)steric interactions dominate (*17, 23, 33*). These are likely to be much more repulsive for *Rhodococcus* C125 than for *Ps. putida* since *Rhodococcus* C125 is coated with highly charged amphiphilic macro-molecules ($\zeta = -50$ mV, at an ionic strength of 0.1 M) whereas *Ps. putida* has a non-polysaccharide cell surface with much less charge ($\zeta = -10$ mV) (*23, 33*). Increased blocking by particle–particle repulsion (*24, 26*) should therefore be much more pronounced for *Rhodococcus* C125 than for *Ps. putida*, which is consistent with our observations.

The different degree in cell–cell repulsion probably also caused the dissimilar deposition behavior of the two strains at coverages close to saturation. The deposition of *Rhodococcus* C125 becomes completely blocked (Figure 3B,C), whereas multilayer attachment and pore-clogging appear to occur for *Ps. putida* (Figure 2).

Both geometric and colloidal factors are consistent with the observation that *Rhodococcus* C125 is an extremely strong and *Ps. putida* is an extremely weak blocking strain. Such bacteria with identical α_0 and contrasting *B* will display a similar initial dispersal in porous media at low applied *c* and low surface coverages. However, great discrepancies will occur at higher coverage that are reached after a prolonged feeding with suspensions low in *c* or shortly after

TABLE 6

Interstitial Fluid Velocity (U/ϵ), Values of Dimensionless Numbers N of Mass Transfer Equation 1, Dimensionless Flux η, and Fractional Contribution (η_{codi}/η) of Sum of Convection and Diffusion to η

strain/collector	experiment	U/ϵ (μm s^{-1})	N_R ($\times 10^{-3}$)	N_{Pe} ($\times 10^4$)	N_G ($\times 10^{-3}$)	N_{vdW} ($\times 10^{-5}$)	η ($\times 10^{-3}$)	η_{codi}/η
Ps. putida/PFA	1 + 3	206	3.1	7.2	1.0	28.4	0.76	0.97
Rhodococcus C125/PFA	4A	225	6.1	15.7	3.5	6.8	0.51	0.85
Rhodococcus C125/PFA	2	155	6.1	10.9	4.9	9.6	0.64	0.87
Rhodococcus C125/PFA	4B	127	6.1	9.9	6.3	12.4	0.71	0.87
Rhodococcus C125/PFA	4C	44	6.1	3.3	16.5	32.7	1.39	0.90
Rhodococcus C125/PTFE	5	221	0.73	104	4.4	8.7	0.15	0.80
Bacillus CB1/sand	ref 13	14	3.1	0.5	13.6	13300	54.4	0.96
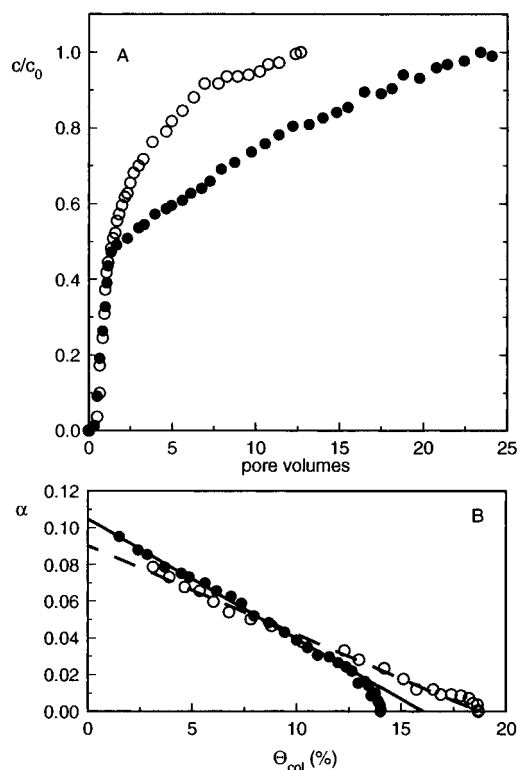
FIGURE 4. Breakthrough of *Bacillus* strain CB1 through columns packed with coarse Texas sand for two different levels of c_0: 3×10^8 cells cm^{-3} (filled symbols) and 1.2×10^9 cells cm^{-3} (open symbols). (A) Breakthrough results as reported by Lindqvist and Enfield (part of Figure 9 in ref 13). (B) The collision efficiency α is given as a function of average surface coverage Θ_{col}; the lines represents the linear regression results; the data with $\Theta_{col} > 13\%$ were excluded from the regression analysis.

applying a high c. Then, strongly blocking cells will be freely transported, whereas weakly blocking cells will start forming multilayered biofilms that eventually will lead to hydraulic head loss and pore-clogging/declogging governing the retention of the bacteria (*11*, *14*).

Applicability of the Collision-Blocking Approach to Natural Porous Media. Part of the data reported by Lindqvist et al. (Figure 9 in ref 13) are replotted in Figure 4A. The $\alpha-\Theta_{col}$ plots are linear and very similar for the two different levels of c (Figure 4B), which indicates that the collision-blocking model applies to this system. The average values of α_0 and B are given in Table 3. Differences in breakthrough at different values of c is a phenomenon that is often observed but not accounted for in conventional microbial transport models (*12–14*, *34*). The occurrence of blocking is further confirmed by the data of Lindqvist and Enfield (*13*). After injection with cell-free groundwater,
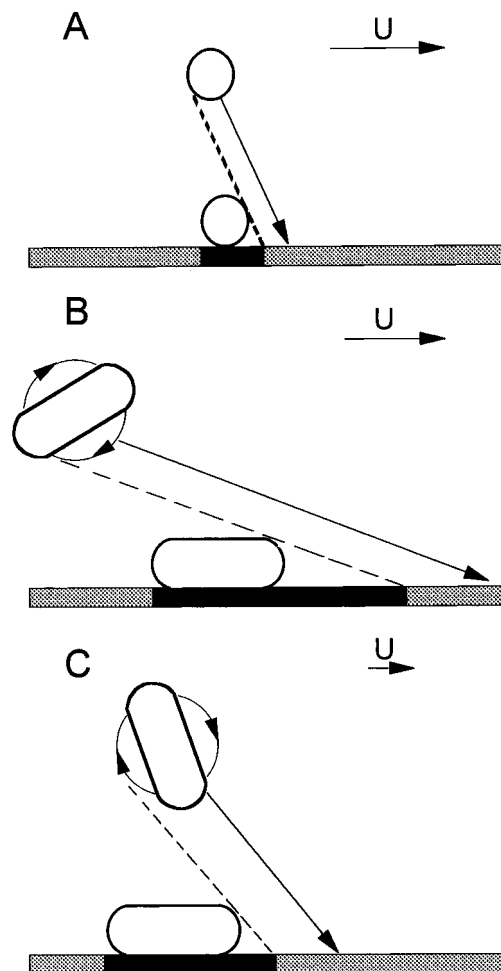
FIGURE 5. Illustration of hydrodynamic effects on blocking illustrated for *Ps. putida* (A) and *Rhodococcus* strain C125 (B) at comparable flow rates and for *Rhodococcus* strain C125 at lower flow rate (C). The blocked area is indicated by a black "shadow".

a repeated feeding of a cell suspension to presaturated columns did not result in any further deposition. It is concluded that the collision-blocking model (eq 3) applies to this system.

The α_0 value of 0.098 obtained from these data is in the range reported for other low ionic strength media (<0.01 M (*35*)), in which electrostatic repulsion inhibits deposition and consequently keeps α_0 low (*5*, *19–21*, *33*). The value for N_{Pe} is rather low (Table 6), and the blocking results can be at best be compared with the *Rhodococcus* C125/PFA system with the lowest flow rate and N_{Pe} value (experiment 4C; Table 6). The levels of B (Table 3) indicate that strain *Bacillus* CB1 is a strongly blocking organism, a feature that is confirmed by the unhindered transport through the sand

columns after surface saturation as observed by Lindqvist and Enfield (*13*). It is likely that electrostatic cell−cell repulsion promoted the blocking in this low ionic strength system.

Conclusion. The collision-blocking deposition equation (eq 3) adequately describes bacterial deposition and transport in coarse grain porous media in cases of strongly blocking cells for all coverages and in case of weakly blocking cells for low coverage conditions. In the next paper, we show that α_0 and B can be related to properties of the cell and solid surface and the ionic strength of the aqueous medium (*36*). Hence, bacteria can be considered as well-characterizable biocolloids of which the mobility in subsurface and other environments can be reliably described and predicted.

Literature Cited

(1) Updegraff, D. M. In *Modeling the environmental fate of microorgansims;* Hurst, C. J., Ed.; American Society of Microbiology: Washington, DC, 1991; pp 1−20.

(2) Bouwer, E. J.; Zehnder, A. J. B. *Trends Biotechnol.* **1993**, *11*, 360−367.

(3) Van der Meer, J. R.; Bosma, T. N. P.; De Bruin, W. P.; Harms, H.; Holliger, C.; Rijnaarts, H. H. M.; Tros, M. E.; Schraa, G.; Zehnder, A. J. B. *Biodegradation* **1992**, *3*, 265−284.

(4) Matthess, G.; Pekdeger, A.; Schroeter, J. *J. Contam. Hydrol.* **1988**, *2*, 171−188.

(5) McDowell-Boyer, L. M.; Hunt, J. R.; Sitar, N. *Water Resour. Res.* **1986**, *22*, 1901−1921.

(6) Lindqvist, R.; Enfield, C. G. *Appl. Environ. Microbiol.* **1992**, *58*, 2211−2218.

(7) Bales, R. C.; Hinkle, S. R.; Kroeger, T. W.; Stocking, K. *Environ. Sci. Technol.* **1991**, *25*, 2088−2095.

(8) Bosma, T. N. P. Ph.D. Thesis, Wageningen Agricultural University, Wageningen, The Netherlands, 1994.

(9) Bouwer, E. J.; Rittmann, B. *Environ. Sci Technol.* **1992**, *26*, 400−401.

(10) Corapcioglu, M. Y.; Haridas, A. *J. Hydrol.* **1984**, *72*, 149−169.

(11) Corapcioglu, M. Y.; Haridas, A. *Adv. Water Res.* **1985**, *8*, 188−200.

(12) Harvey, R. W.; Garabedian, S. P. *Environ. Sci. Technol.* **1991**, *25*, 178−185.

(13) Lindqvist, R.; Enfield, C. G. *Microb. Ecol.* **1992**, *24*, 25−41.

(14) Dickinson, R. A. In *Modeling the environmental fate of microorgansims;* Hurst, C. J., Ed.; American Society of Microbiology: Washington, DC, 1991; 21−47.

(15) Rajagopalan, R.; Tien, C. *J. Am. Inst. Chem. Eng.* **1976**, *22*, 523−533.

(16) Rajagopalan, R.; Tien, C. In *Progress in Filtration and Separation Science*; Wakeman, R. J., Ed.; Elsevier: Amsterdam, 1979; pp 169−268.

(17) Rijnaarts, H. H. M.; Norde, W.; Bouwer, E. J.; Lyklema, J.; Zehnder, A. J. B. *Colloids Surf. B: Biointerfaces* **1995**, *4*, 5−22.

(18) Sjollema, J.; Weerkamp, A. H.; Busscher, H. J. *Biofoul.* **1990**, 1, 101−112.

(19) Elimelech, M.; O'Melia, C. R. *Environ. Sci. Technol.* **1990**, *24*, 1528−1536.

(20) Martin, R. E.; Hanna, L. M.; Bouwer, E. J. *Environ. Sci. Technol.* **1991**, *25*, 2075−2082.

(21) Martin, R. E.; Bouwer, E. J.; Hanna, L. M. *Environ. Sci. Technol.* **1992**, *26*, 1053−1058.

(22) Rijnaarts, H. H. M.; Norde, W.; Bouwer, E. J.; Lyklema, J.; Zehnder, A. J. B. *Appl. Environ. Microbiol.* **1993**, *59*, 3255−3265.

(23) Rijnaarts, H. H. M.; Norde, W.; Lyklema, J.; Zehnder, A. J. B. *Colloids Surf. B: Biointerfaces* **1995**, *4*, 191−197.

(24) Adamczyk, Z.; Siwek, B.; Zembala, M. *Colloids Surf.* **1992**, *62*, 119−130.

(25) Dabros, T.; Van de Ven, T. G. M. *Colloid Polym. Sci.* **1983**, *261*, 694−707.

(26) Dabros, T.; Van de Ven, T. G. M. *Colloids Surf. A: Physicochem. Eng. Aspects* **1993**, *75*, 95−104.

(27) Meinders, J. M.; Noordmans, J.; Busscher, H. J. *J. Colloid Interface Sci.* **1992**, *152*, 265−280.

(28) Sjollema, J.; Busscher, H. J. *Colloids Surf.* **1990**, *47*, 337−352.

(29) Song, L.; Elimelech, M. *Colloids Surf. A: Physicochem. Aspects* **1993**, *73*, 49−63.

(30) Awasaki, T. *J. Am. Water. Works Assoc.* **1937**, *29*, 1591−1602.

(31) Tien, C. *Granular Filtration of Aerosols and Hydrosols*; Butterworth: Stoneham, MA, 1989.

(32) Moran, D. C.; Moran, M. C.; Cushing, R. S.; Lawler, D. F. *J. Am. Water Works Assoc.* **1993**, *85*, 69−93.

(33) Rijnaarts, H. H. M. Ph.D. Thesis, Wageningen Agricultural University, Wageningen, The Netherlands, 1994.

(34) Gannon, J.; Tan, Y.; Baveye, P.; Alexander, M. *Appl. Environ. Microbiol.* **1991**, *57*, 2497−2501.

(35) Stumm, W.; Morgan, J. J. In *Aquatic Chemistry: an Introduction Emphasizing Chemical Equilibria in Natural Waters*; John Wiley & Sons: New York, 1981; pp 599−684.

(36) Rijnaarts, H. H. M.; Bouwer, E. J.; Norde, W.; Lyklema, J.; Zehnder, A. J. B. *Environ. Sci. Technol.* **1996**, *30*, 2877−2883.